International Journal of Information, Control and Computer Sciences
ISSN: 2517-9942
Vol:8, No:7, 2014

Model Predictive 2DOF PID Slip Suppression Control of Electric Vehicle under Braking

Tohru Kawabe

Abstract—In this paper, a 2DOF (two degrees of freedom) PID (Proportional-Integral-Derivative) controller based on MPC (Model predictive control) algorithm for for slip suppression of EV (Electric Vehicle) under braking is proposed. The proposed method aims to improve the safety and the stability of EVs under braking by controlling the wheel slip ratio. There also include numerical simulation results to demonstrate the effectiveness of the method.

Keywords—Model Predictive Control, PID controller, Two degrees of freedom, Electric Vehicle, Slip suppression

I. Introduction

ELECTRIC vehicles (EVs) have received much attention in recent years as a countermeasure to global warming and for being Eco friendly [1], [2], [3], [4].

EVs are automobiles which are propelled by electric motors, using electrical energy stored in batteries or another energy storage devices. Electric motors have several advantages over (internal-combustion engines) ICEs:

(a) Energy efficient.
(b) Environmentally friendly.
(c) Performance benefits.
(d) Reduce energy dependence.

The travel distance per charge for EV has been increased through battery improvements and using regeneration brakes, and attention has been focused on improving motor performance. The following facts are viewed as relatively easy ways to improve maneuverability and stability of EVs.

1) The input/output response is faster than for gasoline/diesel engines.
2) The torque generated in the wheels can be detected relatively accurately
3) Vehicles can be made smaller by using multiple motors placed closer to the wheels.

Much research has been done on the stability of general automobiles, for example, ABS (Anti-lock-Braking Systems), TCS (Traction-Control-Systems), and ESC (Electric-Stability-Control)[5] as well as VSA (Vehicle-Stability-Assist)[6] and AWC (All-Wheel-Control) [7]. What all of these have in common is that they maintain a suitable tire grip margin and reduce drive force loss to stabilize the vehicle behavior and improve drive performance. With gasoline/diesel engines, however, the response time from accelerator input until the drive force is transmitted to the wheels is slow and it is difficult to accurately determine the drive torque, which limits the vehicle's control performance.

This paper deals with the traction control of EV for slip prevention during braking. EVs have a fast torque response and the motor characteristics can be used to accurately determine the torque, which makes it relatively easy and inexpensive to realize high-performance traction control. This is expected to improve the safety and stability of EV under braking.

Several methods have been proposed for the traction control [8], [9], [10] by using slip ratio of EVs, such as the method based on Model Following Control (MFC) in [8] and Sliding Mode Control (SMC) method [11] by us. Moreover, we have been also proposed Model Predictive PID method (MP-PID) in [12]. This method determines the PID controller gain using an MPC algorithm to utilize the capability of explicitly considering the constraints, which is one of the advantages of MPC, to achieve a more advanced and flexible control method[16], [17], [18]. Specifically, the optimum control input is calculated by the MPC explicitly considering the constraints and the PID gain for realizing this is derived in advance newline and used.

PID controllers have a simple construction and have been proved to be practical and highly reliable in many industrial fields[13], [14], [15]. Hence, the merits of MP-PID is that MP-PID controller can be implemented smoothly from conventional PID controller since it still holds PID controller structure. However, there is still room for improving control performance of MP-PID control, especially target-tracking performance, in comparison to standard MPC.

This paper, therefore, proposes model predictive two-degree-of-freedom PID (MP-2DOF PID) control method for slip suppression of EVs under braking improving the safety and stability. The method repeatedly optimizes the control parameters for each control period by solving an optimization problem based on the MPC algorithm, while using the 2DOF PID controller structure. 2DOF PID controller can be implemented by a simple extension of the pre-existing PID controller with feed-forward element. This means MP-2DOF PID inherits the merits of MP-PID, and we can get better performance without much cost. The numerical examples show the effectiveness of the proposed method for slip suppression of EVs under braking.

II. Electric Vehicle Dynamics

As a first step toward practical application, this paper restricts the vehicle motion to the longitudinal direction and uses direct motors for each wheel to simplify the one-wheel model to which the drive force is applied. In addition, braking

T. Kawabe is with the Division of Information Engineering, Faculty of Engineering, Information and Systems University of Tsukuba, Tsukuba 305-8573 JAPAN (phone: +81-29-853-5507; e-mail: kawabe@cs.tsukuba.a.jp).

was not considered this time with the subject of the study being limited to only when driving.

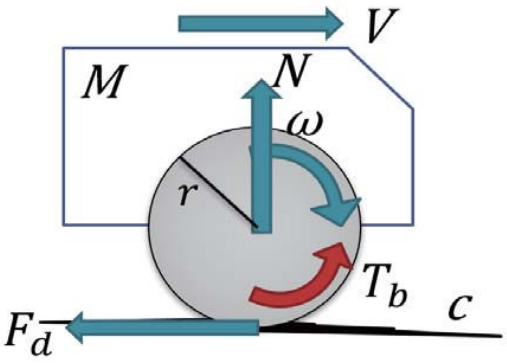

Fig. 1. One-wheel car model

From fig. 1, the vehicle dynamical equations are expressed as (1) to (3).

$$M\frac{dV}{dt} = -F_d(\lambda)+F_a \quad (1)$$

$$J\frac{d\omega}{dt} = rF_d(\lambda)-T_b \quad (2)$$

$$F_d = \mu(c,\lambda)N \quad (3)$$

Where M is the vehicle weight, V is the vehicle body velocity, F_d is the braking force, J is the wheel inertial moment, F_a is the resisting force from air resistance and other factors on the vehicle body, T_b is the braking torque, ω is the wheel angular velocity, r is the wheel radius, c is road surface condition coefficient, and λ is the slip ratio. The slip ratio is defined by (4) from the wheel velocity (V_ω) and vehicle body velocity (V) as

$$\lambda = \frac{V-V_\omega}{V} \quad \text{(braking)}. \quad (4)$$

The frictional forces that are generated between the road surface and the tires are the force generated in the longitudinal direction of the tires and the lateral force acting perpendicularly to the vehicle direction of travel, and both of these are expressed as a function of λ. The frictional force generated in the tire longitudinal direction is expressed as μ, and the relationship between μ and λ is shown by (5) below, which is a formula called the Magic-Formula[19] and which was approximated from the data obtained from testing.

$$\mu(\lambda) = -c\times 1.05\times(e^{45\lambda}-e^{0.45\lambda}) \quad (5)$$

Where c is the coefficient used to determine the road condition and was found from testing to be approximately $c=0.8$ for general asphalt roads, approximately $c=0.5$ for general wet asphalt, and approximately $c=0.12$ for ice roads. For the various road conditions ($0<c<1$), the $\mu-\lambda$ surface is shown in fig. 2. It shows how the friction coefficient μ increases with slip ratio λ ($0.1<\lambda<0.2$) where it attains the maximum value of the friction coefficient. As defined in (3), the braking force also reaches the maximum value corresponding to the friction coefficient. However, the friction coefficient decreases

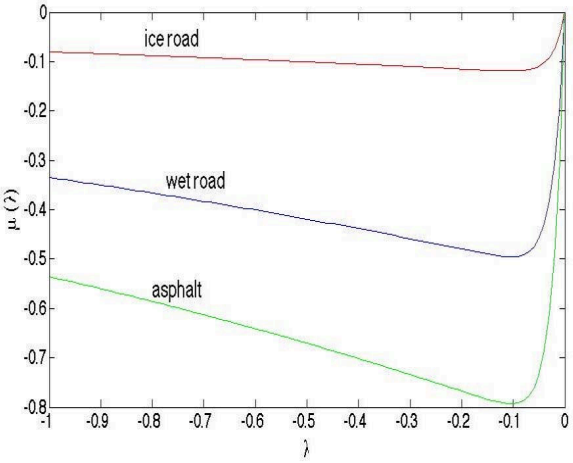

Fig. 2. λ-μ surface for road conditions

to the minimum value where the wheel is completely skidding. Therefore, to attain the maximum value of driving force for slip suppression, it should be controlled the optimal value of slip ratio. the optimal value of λ is derived as follows.

Choose the function $\mu_c(\lambda)$ defined as

$$\mu_c(\lambda) = 1.05\times(e^{45\lambda}-e^{0.45\lambda}). \quad (6)$$

By using (5), (6) can be rewritten as

$$\mu(c,\lambda) = c\cdot\mu_c(\lambda). \quad (7)$$

Evaluating the values of λ which maximize $\mu(c,\lambda)$ for different $c(c>0)$, means to seek the value of λ where the maximum value of the function $\mu_c(\lambda)$ can be obtained. Then let

$$\frac{d}{d\lambda}\mu_c(\lambda) = 0 \quad (8)$$

and solving equation (8) gives

$$\lambda = \frac{log100}{0.45-45} \approx -0.10. \quad (9)$$

Thus, for the different road conditions, when $\lambda\approx-0.10$ is satisfied, the maximum driving force can be gained. Namely, from (5) and fig. 2, we find that regardless of the road condition (value of c), the $\lambda-\mu$ surface attains the largest value of μ when λ is the optimal value -0.10.

III. Introduction of MPC and 2DOF PID control

A. MPC

MPC algorithm is to decide the optimal manipulated values which converge MPC the controlled values to reference values by iteration of optimizing a cost function under constraints. To take advantage of the modern control theory, RHC mainly use the state space model to describe the controlled object. At current time-step k controlled variables $x(k)$ is measured, and MPC controller predict the behavior of the controlled variables sequence from $\hat{x}(k+1)$ to $\hat{x}(k+H_p)$ by the dynamic model of the controlled object described as (10) and (11).

$$x(k+1) = Ax(k)+Bu(k) \quad (10)$$
$$y(k) = Cx(k) \quad (11)$$

The behavior of system depends on future manipulated variables sequence from $\hat{u}(k)$ to $\hat{u}(k+Hp-1)$, that is why MPC controller calculate the sequence $U=[u(k), u(k+1), \cdots, u(k+H_P-1)]$ which makes desired behavior from perspective of cost-minimizing. After calculating, only $\hat{u}(k)$ is inputted to controlled object as current actual input, then, at the next time-step the plant state is sampled again and the prediction and the calculation are repeated. Where H_p is so-called predictive horizon and ^ denotes a predictive value at k. The cost function $J(k)$ at current time-step is given by

$$J(k) = \sum_{i=0}^{H_p-1} \left\{ \| \hat{x}(k+i+1) - x^d \|_Q^2 + \| \hat{u}(k+i) \|_R^2 \right\}. \quad (12)$$

The optimization problem with constraints is given by

$$\min_U J(k) \quad (13)$$

subject to

$$\begin{aligned} x_{min} &\le \hat{x}(k+i) \le x_{max} \\ u_{min} &\le \hat{u}(k+i) \le u_{max} \\ & i = 0, 1, \cdots, Hp. \end{aligned} \quad (14)$$

We assume the controlled object is a multi-input multi-output system, thus $x(k)$ and $u(k)$ are vectors with adequate dimensions. $\| x \|_Q^2$ denotes the quadratic form x^TQx, and x^d reference value and where Q and R are weighting matrices.

B. 2 DOF PID Control

PID is an acronym created from Proportional (proportional action), Integral (integral action), and Derivative (derivative action), and it has a simple structure that makes it easy to intuitively understand the role of each action and thus has been used for many years in a variety of fields and today remains a proved, highly reliable control device used for a variety of subjects.

The control input generated by the standard 1 DOF PID controller in continuous-time is generally expressed by (15).

$$u(t) = K_P e(t) + K_I \int_0^t e(\tau)d\tau + K_D \frac{de(t)}{dt} \quad (15)$$

Where $e(t) := r(t) - y(t)$ (deviation), and where K_P, K_I, and K_D are called the proportional gain, integral gain, and differential gain, respectively.

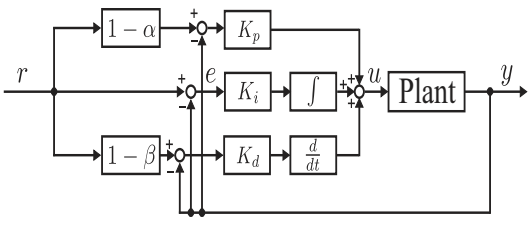

Fig. 3. 2DOF PID control system

As well known, the 2DOF control system naturally has generally advantages over the 1DOF control system. Various 2DOF PID controllers have been proposed for industrial use and also detailed analysis have been made including equivalent transformations, interrelationship with previously proposed variation of 1DOF PID (i.e., the preceded-derivative PID and the I-PD) controllers until now [15].

Although there are various form of 2DOF PID controller, one of the simple form as shown in fig.3 is employed in this paper. Where α $(0 \le \alpha \le 1)$ and β $(0 \le \beta \le 1)$ are feed forward gains.

The control input by this 2DOF PID controller in discrete-time is expressed as follows.

$$\begin{aligned} u(k) &= K_P[(1-\alpha)e(k)] \\ &+ K_I \left[\sum_{i=0}^{k} e(i) \right] \\ &+ K_D[(1-\beta)(e(k) - r(k-1)) + y(k-1)] \end{aligned} \quad (16)$$

IV. MP-2DOF PID CONTROL

For tuning the parameters of 2DOF PID controller by the MPC algorithm, the control input (16) is rewritten as follows.

$$\begin{aligned} \hat{u}(k+j) &= K_P[(1-\alpha)r(k+j) - \hat{y}(k+j)] \\ &+ K_I \left[\sum_{l=0}^{k} e(l) + \sum_{l=1}^{j} \hat{e}(k+l) \right] \\ &+ K_D[(1-\beta)(r(k+j) - \hat{y}(k+j)) \\ &- (1-\beta)r(k+j-1) + \hat{y}(k+j-1)] \end{aligned} \quad (17)$$

where

$$e(k) = r(k) - y(k) \quad (18)$$

Then, the predictive value of $y(k+i)$ is expressed

$$\begin{aligned} \hat{y}(k+i) &= CA^i x \\ &+ \sum_{j=0}^{H_p-1} [CA^{i-1}B, \cdots, CB] [\hat{u}(k), \cdots, \hat{u}(k+i-1)]^T. \end{aligned} \quad (19)$$

The 2DOF-PID controller is determined from (17) by using the set of $\vec{\theta} = (K_P\ K_I\ K_D\ \alpha\ \beta)$ including three feedback PID gains (K_P, K_I, K_D) and two feed-forward gains (α, β),

For tuning of these five MP-2DOF PID gains, we need to solve an optimization problem to get the optimum θ. A weighted square sum with respect to e and u within the prediction horizon H_p is generally used as t he objective function. Here, the objective function J_{LQ} is given as

$$J_{LQ} = \sum_{i=1}^{H_p} q_i \hat{e}^2(k+i) + \sum_{j=0}^{H_p-1} r_j \hat{u}^2(k+j). \quad (20)$$

In (20), e is evaluated at each time-step $k, k+1, \cdots, k+H_p$ and u is evaluated at each control interval $k, k+N_c-1, k+2N_c-1, \cdots, k+H_p$. By using state space model, (10) and (11), repeatedly, we can express $\hat{r}(k+1), \cdots, \hat{r}(k+H_p)$, $\hat{y}(k+1), \cdots, \hat{y}(k+H_p)$, $\hat{e}(k), \cdots, \hat{e}(k+H_P)$, $\hat{u}(k), \hat{u}(k+H_p)$ and J_{LQ}

by $\vec{\theta}$. As a result, the controller design problem at step k is formulated as follows,

$$\min_{\theta} J_{LQ}(\theta) \quad (21)$$
$$s.t. \quad (18) \text{ and } (19)$$
$$j = 0, \cdots, H_p - 1; \quad i = 1, \cdots, H_p.$$

Equation (21) can be solved by some optimization method (for example, the grid search to the discretized θ). Once optimum θ at k is obtained, optimum $u(k) = \hat{u}(k)$ is calculated by (17). We may note, in passing, that values of α and β are fixed to 0, it's standard 1DOF PID controller. The proposed method, therefore, includes 1DOF MP-PID controller design.

V. Numerical Experiments

In order to verify the performance of the proposed method, we compare it with no control using several values of initial velocity (V_0) and mass (M) in (25) on the test course.

A. Experimental setup

Firstly, as shown by (1) $\sim$ (3), the vehicle model has nonlinear characteristics and it's difficult to apply the proposed method to this model as it is. Therefore, a linear approximated model as the perturbed system in the time ($t = k$) is used. If we use the slip ratio in the time $t = k$ as λ_k, and the $\lambda - \mu$ curve inclination in λ_k as

$$a = \frac{d\mu}{d\lambda}\Big|_{\lambda_k}, \quad (22)$$

and using (1) $\sim$ (3), the relation of variation of the slip ratio $\Delta\lambda$ and variation of the motor torque ΔT_m is expressed as follows.

$$\frac{\Delta\lambda}{\Delta T_m} = \frac{M(1-\lambda_k)}{aN\left[M(1-\lambda_k) + \frac{J}{r^2}\right]} \times \frac{1}{\tau_a s + 1} \quad (23)$$

where

$$\tau_a := \frac{J\omega M(1-\lambda_k)}{arN\left[M(1-\lambda_k) + \frac{J}{r^2}\right]} \quad (24)$$

The transfer function is numerically realized using the application software, *Matlab*(*Ver.*8.1.0.604) as the continuous-time state space of the SISO (Single Input Single Output) system. Furthermore, the continuous-time state space model is transformed to the discrete-time state space model with the sampling time $T_s = 0.01$ sec. by *Matlab*.

TABLE I
Parameters used in the simulations

M: Mass of vehicle	1100$[kg]$
J_w: Inertia of wheel	21.1/4 $[kg/m^2]$
r: Radius of wheel	0.26$[m]$
λ^*: Reference slip ratio	0.13
g: Acceleration of gravity	9.81$[m/s^2]$

The variations in initial velocity V_0 and mass of vehicle M are defined as follows.

$$V_{0-min}(= 40[km/h]) \leq V_0 \leq V_{0-max}(= 100[km/h])$$
$$M_{min}(= 1100[kg]) \leq M \leq M_{max}(= 1800[kg]) \quad (25)$$

We use a test course as shown in Table.II as one example in this simulation. This course is assumed as the winter traffic condition of a typical snowy district in the daytime.

TABLE II
Road surface conditions of test course

road length $[m]$	value of c	situation
0 $\sim$ 25	0.12	icy road
25 $\sim$ 50	0.5	wet asphalt
50 $\sim$ 75	0.12	icy road
75 $\sim$ 100	0.8	dry asphalt
100 $\sim$	0.12	icy road

The simulation environment is shown in Table III.

TABLE III
Simulation environment

CPU	Intel(R) Core(TM) i5 2.70GHz
RAM	16.00GB
OS	Mac OS X 10.8.5
Software	MATLAB 7.14.0.739 (R2012a)

B. Simulation result I ($M = 1100$ [Kg])

Table IV shows the stopping (braking) distances and stopping times on the test course with $M = 1100$[Kg].

TABLE IV
Stopping distance and time

V_0	proposed method	no control
40$[km/h]$	31.7[m]/ 4.26[s]	40.2[m]/ 6.63[s]
60$[km/h]$	47.6[m]/ 4.63[s]	88.2[m]/10.30[s]
100$[km/h]$	114.0[m]/ 9.73[s]	355.5[m]/29.05[s]

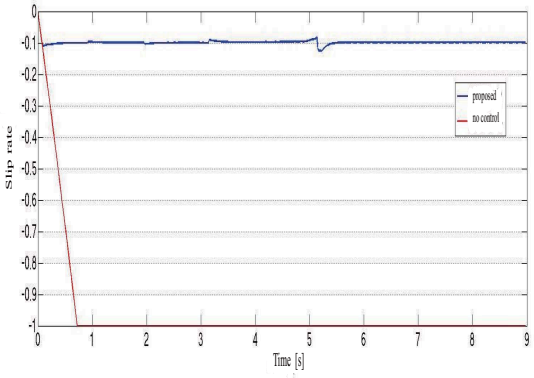

Fig. 4. Time response of slip rate(λ) with $V_0 = 100[km/h]$

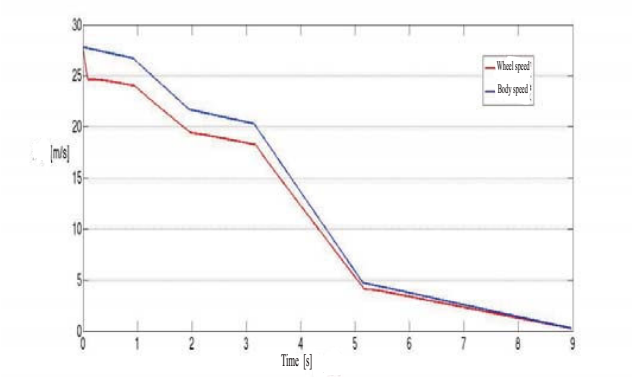

Fig. 5. Time response of body speed (V) and wheel speed(ω) with proposed control ($V_0 = 100[km/h]$)

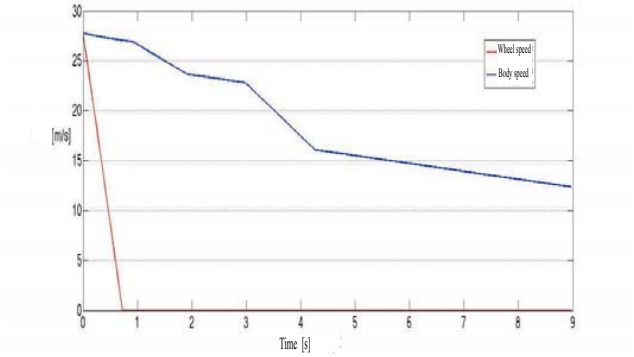

Fig. 6. Time response of body speed (V) and wheel speed(ω) without control ($V_0 = 100[km/h]$)

From table. IV, we can see that the proposed method shows good performance in all initial velocity compared with no control case.

Fig. 4 shows time response of slip rate. From this figure, we can see that the proposed control method can keep the value of λ to almost around -0.1 in any situations. On the other hand, the slip rate gradually decreases without control.

Figs. 5 and 6 show time responses of body speed and wheel speed with proposed method and without control respectively. From fig. 5, we can see that the difference between body and wheel speed is small. On the other hand, from fig. 6, the difference is very big from initial time and tire spinning may be occurs.

C. Simulation result II ($M = 1500$ [Kg])

Table V shows the stopping (braking) distances and stopping times on the test course with $M = 1500$[Kg]. The proposed method also show good performance in this case.

Fig. 7 shows time response of slip rate. From this figure, we can see that the proposed control method can also keep the value of λ to almost around -0.1 in any situations. On the other hand, the slip rate gradually decreases without control.

TABLE V
STOPPING DISTANCE AND TIME

V_0	proposed method	no control
40[km/h]	32.7[m]/ 4.45[s]	49.1[m]/ 8.51[s]
60[km/h]	48.9[m]/ 4.88[s]	113.2[m]/14.48[s]
100[km/h]	117.5[m]/10.30[s]	355.5[m]/25.18[s]

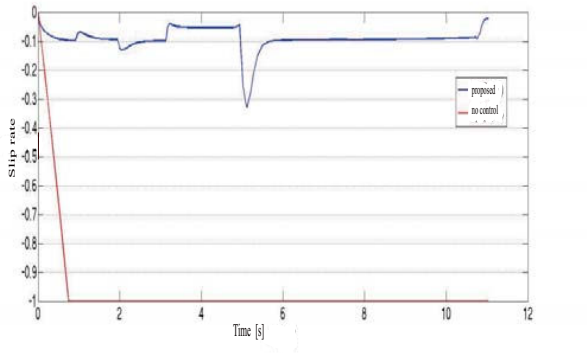

Fig. 7. Time response of slip rate(λ) with $V_0 = 100[km/h]$

D. Simulation result III ($M = 1800$ [Kg])

Table V shows the stopping (braking) distances and stopping times on the test course with $M = 1800$[Kg]. The proposed method also show good performance in this case.

TABLE VI
STOPPING DISTANCE AND TIME

V_0	proposed method	no control
40[km/h]	33.5[m]/ 4.52[s]	56.7[m]/ 9.92[s]
60[km/h]	49.8[m]/ 5.27[s]	127.8[m]/15.16[s]
100[km/h]	121.1[m]/10.93[s]	371.0[m]/29.33[s]

Fig. 8 shows time response of slip rate. From this figure, we can see that the proposed control method can keep the value of λ to almost around -0.1 in any situations. On the other hand, the value of slip ratio is big different from reference value (-0.1) without control.

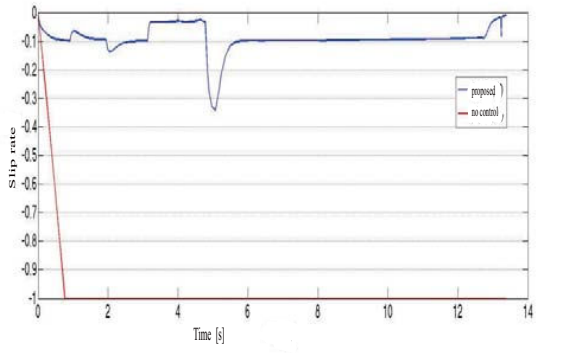

Fig. 8. Time response of slip rate(λ) with $V_0 = 100[km/h]$

VI. Conclusion

This paper proposes MP-2DOF PID control method that focuses on slip suppression for EV traction control under braking situations. The control objective focused on suppressing the slip ratio to the desired value with the variation in the road condition and vehicle mass during the braking.

We can verified that the the proposed method shows good performance. We can also confirm that it is an easy way to improve the control performance without much cost by expanding PID controller to 2DOF PID controller.

As future works, we needed to be considered for saving the energy conservation with all driving situations with acceleration and deceleration and also to be considered the relation with the regenerated braking system. Even for this issue, however, the basic framework of the proposed method can be used as is and can also be expanded relatively easily to form a foundation for making practical EV high performance and safety traction control systems and promoting further progress.

ACKNOWLEDGMENTS

This research was partially supported by Grant-in-Aid for Scientific Research (C) (Grant number: 24560538; Tohru Kawabe; 2012-2014) from the Ministry of Education, Culture, Sports, Science and Technology of Japan.

References

[1] S. Brown, D. Pyke and P. Steenhof, "Electric vehicles: The role and importance of standards in an emerging market", *Energy Policy*, Vol.38, Issue 7, 2010, pp. 3797–3806.
[2] H. Mousazadeh, A. Keyhani, H. Mobli, U. Bardi, G. Lombardi and T. Asmar, "Environmental assessment of RAMseS multipurpose electric vehicle compared to a conventional combustion engine vehicle ", *Journal of Cleaner Production*, Vol.17, Issue 9, 2009, pp. 781–790.
[3] T. Hirota, M. Ueda and T. Futami, "Activities of Electric Vehicles and Prospect for Future Mobility", *Journal of The Society of Instrument and Control Engineering* , Vol.50, 2011, pp. 165–170 (in Japanese).
[4] K. Kondo, "Technological Overview of Electric Vehicle Traction", *Journal of The Society of Instrument and Control Engineering* (in Japanese), Vol.50, 2011, pp. 171–177.
[5] A.T. Zanten, R. Erhardt and G. Pfaff, "VDC; The Vehicle Dynamics Control System of Bosch", *Proc. Society of Automotive Engineers International Congress and Exposition*, 1995, Paper No. 950759.
[6] K. Kin, O. Yano and H. Urabe, Enhancements in Vehicle Stability and Steerability with VSA, *Proc. JSME TRANSLOG 2001*, 2001, pp.407–410 (in Japanese).
[7] K. Sawase, Y. Ushiroda and T. Miura, Left-Right Torque Vectoring Technology as the Core of Super All Wheel Control (S-AWC), *Mitsubishi Motors Technical Review* , No.18, 2006, pp.18–24 (in Japanese).
[8] S. Kodama, L. Li and H. Hori, "Skid Prevention for EVs based on the Emulation of Torque Characteristics of Separately-wound DC Motor", *Proc. The 8th IEEE International Workshop on Advanced Motion Control* , VT-04-12, 2004, pp.75–80.
[9] M. Mubin, S. Ouchi, M. Anabuki and H. Hirata, Drive Control of an Electric Vehicle by a Non-linear Controller, *IEEJ Transactions on Industry Applications* , Vol.126, No.3, 2006, pp.300–308 (in Japanese).
[10] K. Fujii and H. Fujimoto, "Slip ratio control based on wheel control without detection of vehicle speed for electric vehicle", *IEEJ Technical Meeting Record*, VT-07-05, 2007, pp.27–32 (in Japanese).
[11] Li, S., Nakamura, Kawabe, T. and K., Morikawa, 2012. A Sliding Mode Control for Slip Ratio of Electric Vehicle, *Proc. of SICE Annual Conference 2012*, pp.1974–1979.
[12] Kawabe, T., Kogure, Y., Nakamura, K., Morikawa, K. and Arikawa, Y., 2011. Traction Control of Electric Vehicle by Model Predictive PID Controller, *Transaction of JSME Series C*, Vol. 77, No. 781, pp. 3375–3385 (in Japanese).
[13] K.J. Åström and T. Hagglund, "*Advanced PID Control*", The Instrumentation, Systems, and Automation Society, 2005.
[14] A. O'Dwyer, "*Handbook of PI and PID controller tuning rules*", Imperial College Press, 2006.
[15] Araki, M. and Taguchi, T., 2003. Two-Degree-of Freedom PID Controllers, *International Journal of Control, Automation, and Systems*, Vol.1, No.4, pp.401–411.
[16] J.M. Maciejowski, *Predictive Control with Constraints*, (Trans. by Adachi,S. and Kanno,M.), Tokyo Denki University Press, 2005 (in Japanese).
[17] E. F. Camacho and C. Bordons, "*Model Predictive Control* (Advanced Textbooks in Control and Signal Processing) ", Springer-Verlag, 2004.
[18] L. del Re, F. Allgöwer, L. Glielmo, C. Guardiola, I. Kolmanovsky, "*Automotive Model Predictive Control: Models, Methods and Applications* (Lecture Notes in Control and Information Sciences) ", Springer-Verlag, 2010.
[19] H.B. Pacejka and E. Bakker, "The Magic Formula Tire Model", *Vehicle system dynamics*, Vol.21, 1991, pp.1–18.